### Absorption, Metabolism, and Excretion of <sup>14</sup>C-Emvododstat Following Repeat Daily Oral Dose Administration in Human Volunteers Using a Combination of Microtracer Radioactivity and High-Radioactivity Doses

Jiyuan Ma, Oscar L. Laskin, Ad F. Roffel, Wouter H.J. Vaes, Bowen Tang, Jeroen Kolnaar, Kylie O'Keefe, Lee Golden, and © Ronald Kong

PTC Therapeutics, Inc., South Plainfield, New Jersey (J.M., O.L.L., B.T., K.O'K., L.G., R.K.); ICON plc, Groningen, The Netherlands (A.F.R., J.K.); and Netherlands Organization for Applied Scientific Research, Leiden, The Netherlands (W.H.J.V.)

Received July 29, 2023; accepted October 10, 2023

#### **ABSTRACT**

Emvododstat is a potent inhibitor of dihydroorotate dehydrogenase and is now in clinical development for the treatment of COVID-19 and acute myeloid leukemia. Since the metabolism and pharmacokinetics of emvododstat in humans is time dependent, a repeat-dose study design using a combination of microtracer radioactivity and high-radioactivity doses was employed to evaluate the metabolism and excretion of emvododstat near steady state. Seven healthy male subjects each received 16 mg/0.3 µCi <sup>14</sup>C-emvododstat daily oral doses for 6 days followed by a 16 mg/100  $\mu\text{Ci}$  high-radioactivity oral dose on Day 7. Following the last 16 mg/0.3 μCi <sup>14</sup>C-emvododstat dose on Day 6, total radioactivity in plasma peaked at 6 hours postdose. Following a high-radioactivity oral dose (16 mg/100  $\mu$ Ci) of <sup>14</sup>C-emvododstat on Day 7, both whole blood and plasma radioactivity peaked at 6 hours, rapidly declined from 6 hours to 36 hours postdose, and decreased slowly thereafter, with measurable radioactivity at 240 hours postdose. The mean cumulative recovery of the administered dose was 6.0% in urine and 19.9% in feces by 240 hours postdose, and the mean extrapolated recovery to infinity was 37.3% in urine and 56.6% in feces. Similar metabolite profiles were observed after repeat daily microtracer radio-activity oral dosing on Day 6 and after a high-radioactivity oral dose on Day 7. Emvododstat was the most abundant circulating component, and M443 and O-desmethyl emvododstat glucuronide were the major circulating metabolites; M474 was the most abundant metabolite in urine, whereas O-desmethyl emvododstat was the most abundant metabolite in feces.

#### SIGNIFICANCE STATEMENT

This study provides a complete set of the absorption, metabolism, and excretion data of emvododstat, a potent inhibitor of dihydroor-otate dehydrogenase, at close to steady state in healthy human subjects. The resolution of challenges due to slow metabolism and elimination of a lipophilic compound highlighted in this study can be achieved by repeat daily microtracer radioactivity oral dosing followed by high-radioactivity oral dosing at therapeutically relevant doses.

#### Introduction

Emvododstat, also known as PTC299 (Fig. 1), is an orally bioavailable small molecule originally identified as an inhibitor of the translation of vascular endothelial growth factor A (VEGFA) mRNA (Cao

The study was supported by PTC Therapeutics, Inc.

All authors are employees of PTC Therapeutics, Inc., except that O.L.L. is a former employee of PTC Therapeutics, A.F.R. and J.K. are employees of ICON plc, and W.H.J.V is an employee of Netherlands Organization for Applied Scientific Research.

Part of this work was presented as follows: Roffel A., Ma J., Bolt M., Kolnaar J., van Lier J.J., van der Hoek M., Vermeulen E., van Hoogdalem E.-J., Laskin O.L., and Kong R. An approach to investigating small molecule AME properties in humans using a combination of microtracer radioactivity and regular radioactivity doses. 25th Workshop of the IIS-CED (International Isotope Society – Central European Division); 2022 May 5–6; Bad Soden, Germany.

dx.doi.org/10.1124/dmd.123.001471.

et al., 2016) and was developed as an oncology agent for the treatment of solid tumors (Packer et al., 2015; Bender Ignacio et al., 2016; Weetall, et al., 2016). Later research revealed that emvododstat's mechanism of action is due to its direct and potent inhibition of the dihydroorotate dehydrogenase (DHODH) enzyme, a rate-limiting enzyme in the de novo pyrimidine nucleotide synthesis (Cao et al., 2019). In vitro studies demonstrated that emvododstat is more potent against leukemic malignancies, including acute myeloid leukemia (AML), than against solid tumors (Cao et al., 2019; Branstrom et al., 2022). Emvododstat also showed broad-spectrum antiviral activity, and most importantly, emvododstat potently inhibited viral replication and suppressed induction of inflammatory cytokines in COVID-19 (SARS-CoV-2) cell-based assays (Luban et al., 2021). Based on these results, emvododstat has the potential to address unmet needs in certain cancers and RNA virus infection diseases, where cancer cells or viruses rely on the de novo biosynthesis of pyrimidine nucleotides for survival or rapid proliferation. Emvododstat is now under clinical development for the treatment of AML and for hospitalized patients with COVID-19 infection.

**ABBREVIATIONS:** AME, absorption, metabolism, and excretion; AML, acute myeloid leukemia; AMS, accelerator mass spectrometry; AUC, area under the plasma or blood concentration-time curve; eq, equivalent; FDA, Food and Drug Administration; HPLC, high-performance liquid chromatography; PK, pharmacokinetic; QC, quality control;  $T_{1/2}$ , the terminal elimination half-life;  $T_{max}$ , time to maximum blood or plasma concentration; TRA, total radioactivity.

Fig. 1. Structure of emvododstat and proposed metabolic pathways of emvododstat in human subjects following oral dose administration.

In vitro metabolism studies showed that O-demethylation followed by glucuronidation were the major metabolic pathways for emvododstat; multiple cytochrome P450s appeared to be involved in emvododstat metabolism. Emvododstat and O-desmethyl emvododstat were both inhibitors of CYP2D6 and BCRP transporter, but neither of them was a substrate for common efflux or uptake transporters investigated (Ma et al., 2022a). Following oral administration, emvododstat is bioavailable in mice, rats, dogs, and monkeys; the absorption is generally slow, and the plasma exposure of less pharmacologically active O-desmethyl emvododstat is lower than that of parent emvododstat in rodents but relatively higher in dogs and monkeys (Ma et al., 2022a). Following a single oral dose in rats and dogs, excretion of <sup>14</sup>C-emvododstat-derived radioactivity was faster in dogs than in rats, whereas urinary excretion was minimal (<1% of dose) in both rats and dogs; emvododstat was the dominant radioactive component in rat plasma and feces and was also the dominant radioactive component in dog feces, whereas emvododstat and two of its metabolites (O-desmethyl emvododstat and

M312) were the major circulating components in dog plasma (Ma et al., 2022b).

Emvododstat has been administered to healthy subjects, patients with solid tumors and AML, and hospitalized subjects with COVID-19 infection. Following a single oral dose of emvododstat ranging from 0.03 mg/kg to 3.0 mg/kg in healthy subjects, the mean time to maximum blood or plasma concentration ( $T_{\rm max}$ ) was observed in a range of 3.5–5.3 hours. Although  $C_{\rm max}$  increased in a dose-proportional manner, the mean area under the plasma concentration-time curve (AUC) generally increased more than dose proportionally, with increasing dose from 0.03 to 3.0 mg/kg (Weetall et al., 2016). Plasma exposure of *O*-desmethyl emvododstat in human subjects was low, 1.3%–4.5% of emvododstat AUC after a single oral dose of emvododstat, but this ratio increased to 9.6%–38% after repeat 40 mg twice-daily, 80 mg twice-daily, and 100 mg twice-daily dosing for 28 days in human immunodeficiency virus–infected patients with Kaposi sarcoma (Bender Ignacio et al., 2016). Both emvododstat and *O*-desmethyl emvododstat had long

plasma terminal elimination half-life ( $T_{1/2}$ ), and the  $T_{1/2}$  was dose dependent: longer  $T_{1/2}$  was observed with escalating dose (Weetall et al., 2016).

As advocated by the recent Food and Drug Administration (FDA) draft guidance for human radiolabeled mass balance studies, if the investigational drug and/or active metabolite(s) exhibit time-dependent pharmacokinetics, the subjects should receive a single radiolabeled dose of the drug after reaching steady state with nonradiolabeled doses, and the bioanalysis of the nonradiolabeled moieties at steady state should be conducted to help interpret the results because this approach only evaluates the clearance pathway of the radiolabeled drug (https://www.fda. gov/regulatory-information/search-fda-guidance-documents/clinicalpharmacology-considerations-human-radiolabeled-mass-balance-studies). For such a dosing regimen, however, quantification of nonradiolabeled moieties is not possible for unknown metabolites or if the reference standards of the known metabolites are not readily available. On the other hand, although the absorption, distribution, metabolism, and excretion of the total drug and metabolites (radiolabeled and nonlabeled) may have reached steady state following a single radioactivity dose preceded by repeat dosing with nonradiolabeled drug since the overall quantification is based on the radioactivity measurement derived from the last radioactive dose, and the unlabeled parent and metabolites already in the body are not accounted for, such dosing a regimen is still considered as a single radioactive dose. With the increasing application of accelerator mass spectrometry (AMS) technology in pharmaceutical industry, we believe that at the same total therapeutic dose, repeated daily microtracer radioactivity dosing followed by a traditional high-radioactivity dose is a practical and better approach to investigate the absorption, metabolism, and excretion (AME) properties of compounds with nonlinear pharmacokinetics (PK) or for which the metabolism is time dependent. AMS analysis of matrices (plasma, urine, and feces) from the last microtracer radioactivity dosing provides AME properties at or near steady state, whereas liquid scintillation counting of the samples from the traditional higher-radioactivity dose provides rich information, such as mass balance and metabolite formation and elimination kinetics, at a reasonable cost. Here, we report the AME properties of emvododstat in healthy human subjects at close to steady state by applying a dedicated study design that includes repeated daily microtracer radioactivity oral dosing followed by a high-radioactivity oral dose.

#### **Materials and Methods**

#### Chemical

GMP-grade <sup>14</sup>C-emvododstat (25.4 μCi/mg; radiochemical purity and chemical purity >99%) was prepared by Pharmaron (Cardiff, UK). Nonradiolabeled emvododstat (chemical purity >99%) was manufactured by Hovione FarmaCiencia SA (Loures, Portugal), and *O*-desmethyl emvododstat (>97% purity) was synthesized by Siegfried AG (Zofingen, Switzerland).

### Methods

Study Design and Sample Collection. The human AME study was conducted in accordance with the Declaration of Helsinki and the International Council for Harmonization Good Clinical Practice. An independent ethics committee reviewed and approved the clinical study protocol, any clinical study protocol amendments, subject information sheets, written informed consent forms, and other relevant documentation. Prior to participation in the study, each subject was apprised of the nature and purpose of the study, and informed consent was obtained.

Since metabolism of emvododstat in humans appears to be time dependent (Weetall et al., 2016), to evaluate emvododstat metabolism near steady state, a study design using repeat daily oral doses containing microtracer radioactivity followed by a single oral dose with high radioactivity was adopted in this study. Available data from previous clinical studies in healthy volunteers and patients indicated that a dose of up to 80 mg once daily in a tablet formulation is a safe

dose to be used in clinical studies with healthy volunteers. The current study was performed with an oral solution of emvododstat at a dose of 16 mg once daily, which was expected to provide similar exposure to emvododstat as the 40–80 mg once daily in a tablet formulation. The  $0.3~\mu Ci$  or  $11.1~kBq^{-14}C$ -emvododstat microtracer radioactivity dose was projected to be adequate for the detection of emvododstat and its metabolites using AMS. The estimated effective radiation burden after a single oral radioactivity dose of  $100~\mu Ci$  or  $3.7~MBq^{-14}C$ -emvododstat was estimated to be approximately 0.48~mSv. For biomedical investigations in small groups of human volunteers, an effective dose of 0.1–1.0~mSv is considered acceptable per the guidance from the International Commission on Radiologic Protection, User's ICRP publication 60 (https://journals.sagepub.com/doi/pdf/ $10.1177/ANIB_21_1$ -3) and ICRP 103 (https://journals.sagepub.com/doi/pdf/ $10.1177/ANIB_21_2$ -4).

The clinical phase of the study was conducted at ICON (Groningen, the Netherlands). A total of seven healthy male subjects between 19 and 32 years of age and with a body mass index between 20.6 and 28.0 kg/m<sup>2</sup> participated in the study. All subjects were White. On Days 1-6, each subject received a 16 mg (0.3 µCi or 11.1 kBq) once-daily oral dose of <sup>14</sup>C-emvododstat after at least 10 hours of overnight fasting. Following the last oral dose on Day 6, blood samples were collected at 0, 0.5, 1, 1.5, 2, 3, 4, 6, 8, 12, 16, and 24 hours postdose, urine samples were collected from 0 to 12 and from 12 to 24 hours, and fecal samples were collected from 0 to 24 hours in all subjects post Day-6 dose. On Day 7, each subject received a single oral dose of 16 mg (100 μCi or 3.7 MBq) <sup>14</sup>C-emvododstat. Blood samples were collected at 0, 0.5, 1, 1.5, 2, 3, 4, 6, 8, 12, 16, 24, 36, and 48 hours and at 24hour intervals up to 240 hours postdose, and urine and fecal samples were collected continuously and quantitatively over 24-hour intervals up to 240 hours post Day-7 dose. By the 240 hours collection period, none of the subjects met the discharge criteria (≥90% of the dose recovered or <0.5% of the dose excreted in urine and feces combined in two consecutive 24-hour collection intervals), and all subjects were invited for five additional follow-up visits with 24hour urine and feces collection periods: all subjects returned for additional follow-up on Day 23 and Day 30, three subjects on Day 45, and two subjects on Day 59 and Day 73. All plasma, urine, and fecal samples were stored at −70°C until analysis.

Sample Preparation for Total Radioactivity Analysis. Total radioactivity (TRA) in plasma, urine, and fecal samples post Day-6 dose (16 mg/0.3  $\mu$ Ci or 11.1 kBq) was measured using AMS at The Netherlands Organization for Applied Scientific Research (Leiden, The Netherlands). For AMS analysis, a reference-standard Australian National University sucrose-8542 ( $C_{12}H_{22}O_{11}$ ) with a certified  $^{14}C/^{12}C$  isotope ratio was used to check the performance of the instrument; five standard samples and two quality-control (QC) samples were included in each batch analysis, with a minimum of three replicates (van Duijn et al., 2014).

TRA in blood, plasma, urine, and fecal samples post Day-7 dose ( $16 \text{ mg/}100 \mu\text{Ci}$  or 3.7 MBq) was measured using liquid scintillation counting at ICON (Groningen, the Netherlands).

Sample Preparation for Metabolite Profiling and Identification. Following the last  $16 \text{ mg/0.3} \mu\text{Ci}\ ^{14}\text{C}$ -emvododstat dose on Day 6, an equal volume of plasma sample at 0, 0.5, 1, 1.5, 2, 3, 4, 6, 8, 12, 16, and 24 hours was separately pooled across seven subjects first, then a volume that was proportional to the time interval was taken at each timepoint to prepare a 0–24-hour AUC pooled plasma (Hop et al., 1998); a volume that was proportional to individual 0–12- and 12–24-hour urine sample volume was pooled across time intervals and subjects to prepare a single 0–24-hour urine pool, and a weight that was proportional to individual 0–24-hour fecal sample weights was pooled across seven subjects to prepare a single 0–24-hour feces pool.

Following the 16 mg/100  $\mu$ Ci <sup>14</sup>C-emvododstat dose on Day 7, plasma from each subject at 1, 2, 3, 4, 6, 12, 24, 48, 144, and 240 hours was selected and pooled with the same volume by the timepoints across subjects; a volume that was proportional to individual 0–240-hour urine volumes from all seven subjects was combined to prepare a 0–240-hour urine pool, and a weight that was proportional to individual 0–240-hour fecal sample weights was pooled across subjects to prepare a 0–240-hour feces pool.

The pooled Day-6 and Day-7 plasma samples were extracted with acetonitrile (3x, v/v) three times. The acetonitrile extracts were combined and evaporated to dryness under a nitrogen stream, and the residues were reconstituted with acetonitrile:water (70:30, v/v) for radio-profiling. The pooled 0–24-hour Day-6 urine was analyzed directly. A 44-mL aliquot of pooled 0–240-hour urine after the

Day-7 dose was loaded to a Waters Oasis 35CC HLB cartridge that was conditioned with 12 mL of ethanol, followed by 36 mL of water; after sample loading, the cartridge was washed with 36 mL of water, followed by 24 mL of ethanol; the ethanol fraction was evaporated to dryness under a nitrogen stream, and the residue was reconstituted with ethanol:water (1:1, v/v) for radio-profiling. The pooled Day-6 and Day-7 fecal samples were extracted with acetonitrile (3×, v/v) three times; the acetonitrile extracts were combined and evaporated to dryness under a nitrogen stream, and the residues were reconstituted in acetonitrile:water (70:30, v/v) for radio-profiling.

Metabolite Profiling and Identification. The metabolite profiles were determined by high-performance liquid chromatography (HPLC) radio-chromatography using a Waters 2695 or Acquity H-Class UPLC system. An ACE 3 C18 AR column (3  $\mu$ m, 150 × 4.6 mm, maintained at 30°C) and two solvent systems of 0.1% formic acid and 2 mM ammonium acetate in water:acetonitrile (95:5, v/v) (A) and 0.1% formic acid and 2 mM ammonium acetate in acetonitrile:water (95:5, v/v) (B) were used. The flow rate was 0.7 mL/min, and the linear gradients were: 5% B for 3 minutes; 5%–25% B in 2 minutes; 25%–50% B in 25 minutes; 50%–95% B in 10 minutes, hold 95% B for 5 minutes; 95%–100% B in 5 minutes, hold 100% B for 3 minute; and 100%–5% B in 1 minute, hold 5% B for 15 minutes.

HPLC fractions from Day-6 plasma, urine, and feces were collected by time (20.7 s/fraction for plasma; 17.5 s/fraction for urine and feces), and the radioactivity in each fraction was determined by AMS analysis (van Duijn et al., 2014). HPLC fractions from plasma, urine, and feces after the Day-7 dose were collected by time (15 s/fraction) to Deepwell LumaPlate-96 plates. The plates were subsequently dried by a SpeedVac concentrator for up to 8 hours. The radioactivity in each fraction was determined by Packard TopCount NXT Microplate Scintillation and Luminescence Counter technology. HPLC radio-chromatograms were reconstructed, and the radioactivity peaks were integrated to determine the percentage of distribution of individual radioactivity peaks in each sample. Plasma, urine, and fecal metabolites were identified or characterized by liquid chromatography-tandem mass spectrometry using a Thermo Q Extractive mass spectrometer (Thermo Fisher Scientific, Waltham, MA). The O Extractive was equipped with an electrospray ionization source operated in positive or negative ion mode with a capillary temperature of 350°C and spray voltage of 3.5 kV. The sheath gas, auxiliary gas, and sweep gas pressures were 50, 40, and 10 units, respectively.

**Pharmacokinetic Analysis.** PK data were generated by noncompartmental PK analysis using WinNonlin (Version 8.3, Certara Corporation; Princeton, NJ). The following parameters were calculated to the extent possible:  $C_{max}$ ,  $T_{max}$ ,  $T_{1/2}$ , and AUC.

**Safety Analysis.** Safety and tolerability assessments were performed in accordance with the schedule of assessments. Adverse events were recorded from admission on Day -1 until the last 24-hour follow-up visit. Any clinically significant observations in results of clinical laboratory, electrocardiogram, vital signs, or physical examinations were recorded as adverse events (serious and nonserious).

#### Results

#### **Safety Evaluation**

All subjects received 112 mg emvododstat over 7 days (16 mg/day). On Days 1–6, the oral dose contained 0.3  $\mu$ Ci of  $^{14}$ C-emvododstat (1.8  $\mu$ Ci in total), and on Day 7, the oral dose contained 100  $\mu$ Ci of  $^{14}$ C-emvododstat. The administration of a daily oral dose of 16 mg  $^{14}$ C-emvododstat for 7 days to healthy male subjects was found to be safe and well tolerated. All treatment-emergent adverse events were of mild (grade 1) severity. All treatment-emergent adverse events recovered without sequelae. No deaths or other serious adverse events (SAEs) were reported. There were no findings of clinical relevance with respect to clinical laboratory parameters, vital signs, electrocardiograms, or physical examinations.

# Plasma PK and Metabolite Profiles following Repeat Daily Oral $^{14}\mathrm{C\text{-}Emvododstat}$ Dose Administration on Day 6

For AMS analysis, quality control was performed by the triplicate analysis of the QC samples at two different concentrations in each run. The measured  $^{14}\text{C}/^{12}\text{C}$  ratios of the QC samples did not deviate more

than 15% from the true value, and the coefficient of variation was <15% in all runs.

Following once-daily oral dosing of 16 mg/0.3  $\mu$ Ci <sup>14</sup>C-emvododstat for 6 days, TRA in Day-6 plasma increased from 0.14  $\mu$ g equivalent (eq)/mL predose to a maximum of 0.30  $\mu$ g eq/mL at 6 hours postdose. The TRA decreased to a value similar to the predose value by 24 hours postdose (0.16  $\mu$ g eq/mL). The lower limit of quantification for plasma TRA was 0.002  $\mu$ g eq/mL. The plasma TRA concentration-time curve of pooled plasma across seven subjects is depicted in Fig. 2, and the PK parameters are shown in Table 1.

Following once-daily oral dosing of  $16 \text{ mg/0.3} \mu\text{Ci}^{14}\text{C}$ -emvododstat for 6 days, emvododstat was the dominant radioactive component, whereas O-desmethyl emvododstat glucuronide and M443 were the most abundant metabolites in 0–24-hour plasma after the last dose on Day 6. Emvododstat was not detectable, whereas M474 was the dominant metabolite in pooled 0–24-hour urine after the last dose on Day 6. Emvododstat and O-desmethyl emvododstat were the most abundant components in pooled 0–24-hour feces after the last dose on Day 6. The Day-6 plasma metabolite profile is shown in Fig. 3, PK parameters of emvododstat and its metabolites are shown in Table 2, and the metabolite distribution data in urine and feces are summarized in Table 3.

## Blood/Plasma PK, Mass Balance, and Metabolite Profiles following Oral $^{14}\mathrm{C\text{-}Emvododstat}$ Dose on Day 7

Following a single oral 16 mg/100  $\mu$ Ci  $^{14}$ C-emvododstat dose on Day 7, which was preceded by 6 days of daily oral dosing of 16 mg/0.3  $\mu$ Ci  $^{14}$ C-emvododstat, both whole-blood and plasma TRA increased from the first timepoint onwards to reach a mean maximum of 0.11 and 0.19  $\mu$ g eq/mL, respectively, at 6 hours postdose, rapidly declined from 6 hours to 36 hours postdose, and decreased slowly thereafter. TRA in whole-blood and plasma was measurable at 240 hours postdose in all subjects. The mean blood:plasma TRA ratio was similar throughout the sampling period and ranged from 0.55 to 0.62. The plasma and blood TRA concentration-time curves are depicted in Fig. 2, and the PK parameters are shown in Table 1.

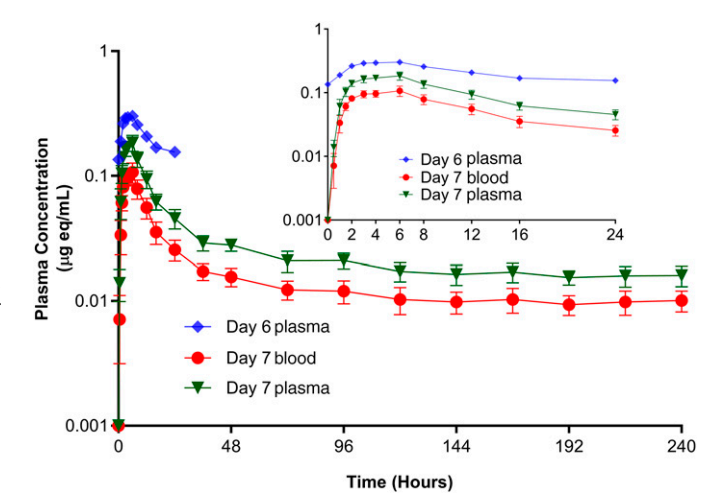


**Fig. 2.** Mean concentration-time curve of total radioactivity in plasma on Day 6 following a 16 mg/0.3 μCi or 11.1 kBq repeat daily oral dose of emvododstat and mean  $\pm$  S.D. concentration-time curves of total radioactivity in blood and plasma following a 16 mg/100 μCi or 3.7 MBq oral dose of emvododstat on Day 7 in healthy male human subjects. Figure insert depicts 0–24-hour time profiles only. The Day-6 profile was generated from AMS analysis after six daily 0.3 μCi doses. Day 7 profile was generated from scintillation counting after six daily 0.3 μCi doses and a 100 μCi dose on Day 7. The total radioactivity after repeated 0.3 μCi daily dosing was too low to affect the scintillation counting results. Thus, the Day-7 profile was considered a single-dose profile.

TABLE 1

Pharmacokinetic parameters of <sup>14</sup>C-emvododstat-derived radioactivity in 0-24-hour plasma on Day 6 following a 16 mg/0.3 µCi or 11.1 kBq repeat daily oral dose of emvododstat and in blood and plasma following a 16 mg/100 µCi or 3.7 MBq oral dose of emvododstat on Day 7 in healthy male human subjects

PK Parameters	Day 6 (Plasma) 0–24-hour pool (N = 7)	Day 7 (Plasma) Mean $\pm$ S.D. (N = 7)	Day 7 (Whole Blood) Mean ± S.D. (N = 7)
C <sub>max</sub> (μg eq/mL)	0.30	$0.19 \pm 0.03$	0.11 ± 0.02
$T_{max}(h)$	6	6 (3–6) <sup>a</sup>	6 (3–6) <sup>a</sup>
$T_{1/2}$ (h)	NC	NC	NC
$AUC_{0-24}$ (µg eq·h/mL)	5.08	$2.31 \pm 0.26$	$1.35 \pm 0.19$
AUC <sub>0-240</sub> (μg eq·h/mL)	NA	$6.60 \pm 0.80$	$3.90 \pm 0.57$
AUC <sub>0-∞</sub> (μg eq·h/mL)	NC	NC	NC

 $AUC_{0-24}$ , area under the concentration-time curve from time zero to 24 hours postdose;  $AUC_{0-240}$ , area under the concentration-time curve from time zero to 240 hours postdose;  $AUC_{0-\infty}$ , area under the concentration-time curve from time 0 to the infinity; NA, not applicable; NC, not calculable.

<sup>a</sup>T<sub>max</sub> is median (min-max).

By 240 hours after the  $16 \text{ mg/}100 \,\mu\text{Ci}^{-14}\text{C}$ -emvododstat dose on Day 7, a mean of 6.0 and 19.9% of the administered dose was recovered in urine and feces, respectively. The mean amount of TRA excreted in urine in each 24-hour interval increased with time to reach a maximum mean excretion during the first follow-up collection interval (384–408 hours postdose). After this time, the mean radioactivity in urine decreased during each consecutive 24-hour collection period. Excretion of TRA in feces started within 24 hours postdose, reached a maximum during the 24–48-hour interval, and showed a slow decrease from the 120–144-hour interval onwards. This decrease continued until the last collection interval. The mean combined excretion in urine and feces was 0.5% of the dose on Days 59 to 60 and was 0.4% of the dose on Days 73 to 74, the last follow-up visit. Based on (log) linear excretion rate constants, the mean extrapolated excretion from 0 hours to infinity was calculated. The mass balance data are summarized in Table 4.

Following a single oral 16 mg/100  $\mu$ Ci  $^{14}$ C-emvododstat dose on Day 7, which was preceded by 6 days of daily oral dosing of 16 mg/0.3  $\mu$ Ci  $^{14}$ C-emvododstat, the plasma metabolite profiles were similar to those following the last 16 mg/0.3  $\mu$ Ci  $^{14}$ C-emvododstat dose on Day 6. The representative metabolite profiles are shown in Fig. 3, the plasma concentration-time curves of TRA and the most prominent emvododstat metabolites are shown in Fig. 4, PK parameters are shown in Table 2, and the metabolite distribution data in urine and feces are summarized in Table 3.

#### **Metabolite Identification**

In addition to unchanged emvododstat, eight metabolites were identified or characterized in plasma, urine, or feces after oral administration of <sup>14</sup>C-emvododstat.

Emvododstat and *O*-desmethyl emvododstat were identified by direct comparison of HPLC retention times and high-resolution mass spectral data with reference standards. Structures of other metabolites were proposed based on their high-resolution mass spectral data of chlorine isotopic patterns and fragmentation ions relative to emvododstat or *O*-desmethyl emvododstat. Proposed structures and metabolic pathways for the formation of the detected metabolites are presented in Fig. 1.

**Emvododstat.** The observed accurate mass for the protonated molecular ion (MH $^+$ ) of emvododstat was at m/z 467.0923 (calculated 467.0924 with a formula of  $C_{25}H_{21}O_3N_2Cl_2^+$ ). The characteristic product ion at m/z 359.0350 was due to the neutral loss of the anisole moiety ( $C_7H_8O$ ) and at m/z 121.0649 ( $C_8H_9O^+$ ) was attributed to the 4-methoxyphenylmethylium ion.

*O*-Desmethyl Emvododstat. The observed accurate mass for MH $^+$  of *O*-desmethyl emvododstat was at m/z 453.0765 (calculated 453.0767 with a formula of  $C_{24}H_{19}O_3N_2Cl_2^+$ ). The characteristic product ion at m/z 359.0353 was due to the neutral loss of the phenol moiety ( $C_6H_6O$ )

and at m/z 107.0494 ( $C_7H_7O^+$ ) was attributed to the 4-hydroxyphenyl-methylium ion.

*O*-Desmethyl Emvododstat Glucuronide. The observed accurate mass for MH $^+$  of *O*-desmethyl emvododstat glucuronide was at m/z 629.1086 (calculated 629.1088 with a formula of  $C_{30}H_{27}O_9N_2Cl_2^+$ ), which is 176.0321 Da ( $C_6H_8O_6$ ) higher than *O*-desmethyl emvododstat, indicating a glucuronic acid conjugate of *O*-desmethyl emvododstat. The characteristic product ions at m/z 453.0770, 359.0350, and 107.0493 all agreed well with *O*-desmethyl emvododstat glucuronide.

**M312.** The observed accurate mass for MH $^+$  of M312 was at m/z 313.1098 (calculated 313.1102 with a formula of  $C_{18}H_{18}ON_2Cl^+$ ), which is 153.9822 Da ( $C_7H_3O_2Cl$ ) lower than emvododstat, indicating the neutral loss of the 4-chlorophenyl formate moiety due to the amide bond hydrolysis. The characteristic product ions at m/z 205.0530 ( $C_{11}H_{10}ClN_2^+$ ) and 121.0648 also agreed well with the proposed structure.

**M298.** The observed accurate mass for MH $^+$  of M298 was at m/z 299.0945 (calculated 299.0946 with a formula of  $C_{17}H_{16}ON_2Cl$ ), which is 153.9822 Da ( $C_7H_3O_2Cl$ ) lower than O-desmethyl emvododstat, or 14.0157 Da (CH $_2$ ) lower than M312, indicating the neutral loss of the 4-chlorophenyl formate moiety due to the amide bond hydrolysis from O-desmethyl emvododstat or demethylation from M312. The characteristic product ions at m/z 205.0530 and 107.0492 also agreed well with the proposed structure.

**M474.** The observed accurate mass for MH $^+$  of M474 was at m/z 475.1265 (calculated 475.1267 with a formula of  $C_{23}H_{24}O_7N_2Cl^+$ ), which is 176.0321 Da ( $C_6H_8O_6$ ) higher than M298, indicating a glucuronic acid conjugate of M298. The characteristic product ions at m/z 299.0946, 205.0530, and 107.0492 also agreed well with the proposed structure.

**M324.** The observed accurate mass for MH $^+$  of M324 was at m/z 325.0736 (calculated 325.0738 with a formula of  $C_{18}H_{14}O_2N_2Cl^+$ ), which is 11.9636 Da (1 oxygen minus 4 hydrogens) higher than M312, indicating that M324 could be an oxidation and dehydrogenation metabolite of M312. The product ions at m/z 310.0503 of  $(C_{17}H_{11}O_2N_2Cl^+)$ , 282.0554  $(C_{16}H_{11}ON_2Cl^+)$ , and 253.0605  $(C_{15}H_{10}N_2Cl^+)$  were observed.

**M443.** The observed accurate mass for MH $^+$  of M443 was at m/z 444.1318 (calculated 444.1321 with a formula of  $C_{22}H_{23}O_5N_3Cl^+$ ). Compared with emvododstat, the characteristic product ions of M443 at m/z 357.0999 ( $C_{19}H_{18}N_2O_3Cl^+$ ) and 121.0648 ( $C_8H_9O^+$ ) suggest that the tetrahydro-2H-pyrido[3,4-b]indole-2-carboxylate and 4-methoxyphenyl moieties are intact, indicating the modification of the 4-chlorophenyl moiety of emvododstat. The observed product ions of M443 at m/z  $106.0499~(C_3H_8NO_3^+)$ ,  $88.0392~(C_3H_6NO_2^+)$ , and  $60.0444~(C_2H_6NO^+)$  are characteristic of serine-derived ion species, indicating that M443 could be a serine conjugate product following the ester bond hydrolysis of emvododstat.

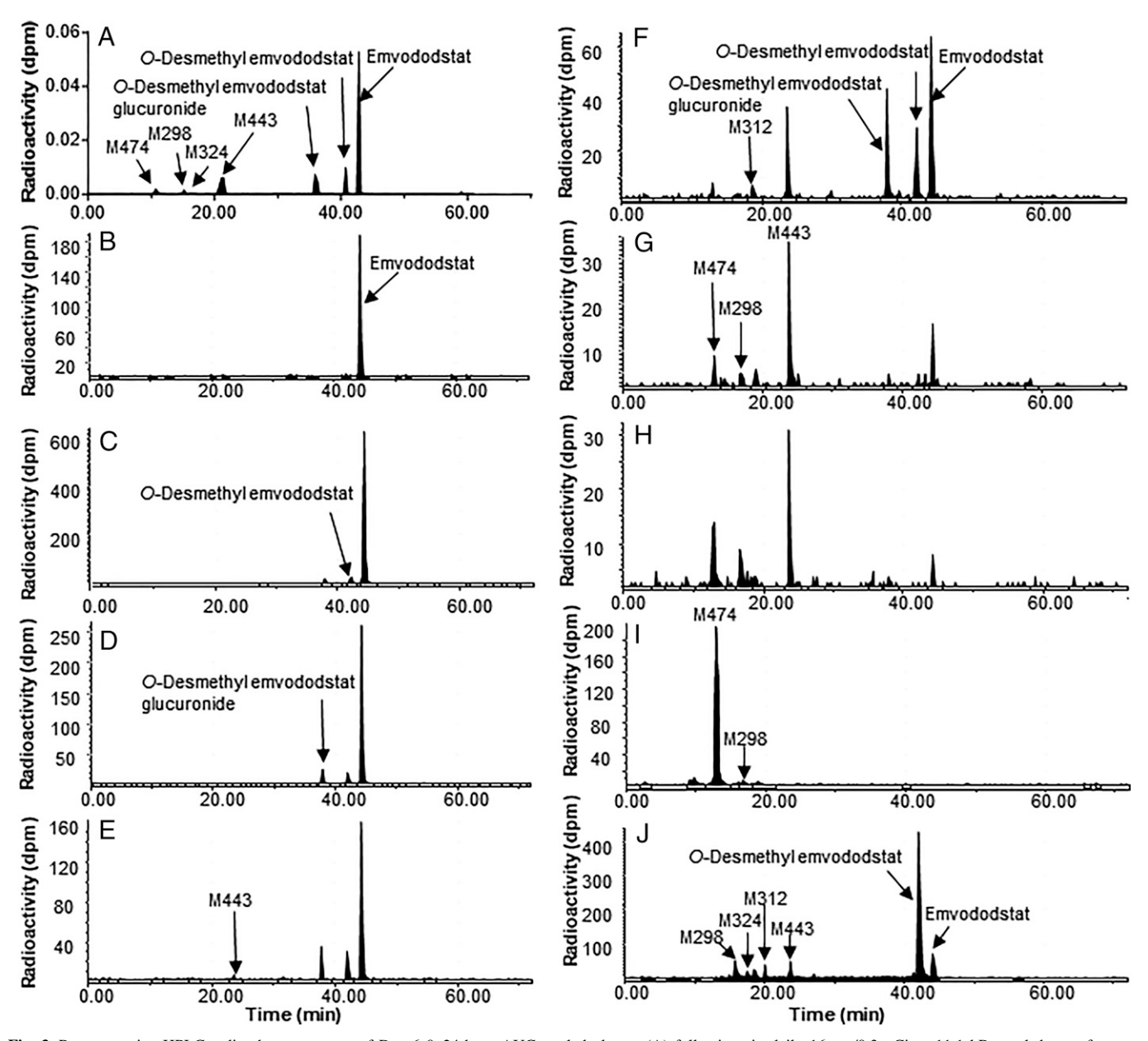


Fig. 3. Representative HPLC radio-chromatograms of Day-6 0–24-hour AUC pooled plasma (A) following six daily 16 mg/0.3 µCi or 11.1 kBq oral doses of emvododstat and 1 hour (B), 3-hour (C), 6-hour (D), 12-hour (E), 48-hour (F), 144-hour (G), and 240-hour (H) pooled plasma, 0–240-hour pooled urine (I), and 0–240-hour pooled feces (J) following a 16 mg/100 µCi or 3.7 MBq oral dose of emvododstat on Day 7 in male healthy subjects.

**M482.** The observed accurate mass for MH $^+$  of M482 was at m/z 483.0875 (calculated 483.0873 with a formula of  $C_{25}H_{21}O_4N_2Cl_2^+$ ), which is 15.9949 Da (one oxygen) higher than emvododstat, indicating that M482 was a mono-oxidation metabolite of emvododstat.

### Discussion

Emvododstat is a lipophilic, neutral compound with low aqueous solubility. Following a single oral dose in male Long-Evans rats, distribution of <sup>14</sup>C-emvododstat–derived radioactivity was extensive, with the endocrine, fatty, and secretory tissues containing the highest radioactivity (Ma et al., 2022b). Consistent with extensive distribution and retention in fatty tissues in male Long-Evans rats, excretion of <sup>14</sup>C-emvododstat–derived radioactivity in intact male Sprague-Dawley rats was slow following a single oral dose, approximately 65% of the dose (0.3% in urine and 54.7% in feces, whereas 35.4% in carcass)

within 7 days postdose in rats. In contrast, approximately 93% of dose was recovered by 8 days postdose, with most of the radioactivity excreted in 0–24-hour feces following a single oral dose in dogs. The faster excretion in dogs was most likely due to lower absorption as indicated by the observation that close to 80% of dose was excreted in 0–24-hour feces, and >94% of fecal radioactivity was attributed to unchanged emvododstat, with little contribution from metabolites (Ma et al., 2022b).

Following a single oral 16 mg/100  $\mu$ Ci  $^{14}$ C-emvododstat dose on Day 7 in human subjects in the current study, approximately 26% of the dose (6% in urine and 19.9% in feces) was recovered by 240 hours postdose. Additional 24-hour collection intervals were used to follow up the excretion until 1608 hours postdose. The total recovery as extrapolated to infinity in the current study was 94.7% (37.3% in urine and 56.6% in feces) (Table 4). Urinary excretion of  $^{14}$ C-emvododstat–derived radioactivity was low in both rats and dogs (<1% dose within 8 days post

TABLE 2 Pharmacokinetic parameters of total radioactivity, emvododstat, and its metabolites in pooled plasma following oral administration of <sup>14</sup>C-emvododstat in healthy male human subjects

Day	Dose	Component	T <sub>max</sub> (h)	T <sub>1/2</sub> (h)	T <sub>last</sub> (h)	$\begin{array}{c} C_{max} \\ (\mu g \ eq/mL) \end{array}$	$\begin{array}{c} AUC_{0-24} \\ (\mu g \ eq \cdot h/mL) \end{array}$	AUC <sub>0-240</sub> (μg eq·h/mL)	% AUC <sup>a</sup> of TRA
6	16 mg/0.3 μCi <sup>b</sup>	TRA	6	NC	24	0.30	5.08	NA	100
		Emvododstat	NA	NA	NA	NA	2.59	NA	51.0
		O-Desmethyl emvododstat	NA	NA	NA	NA	0.49	NA	9.6
		M298	NA	NA	NA	NA	0.11	NA	2.2
		M443	NA	NA	NA	NA	0.72	NA	14.1
		M474	NA	NA	NA	NA	0.17	NA	3.4
		O-Desmethyl emvododstat glucuronide	NA	NA	NA	NA	0.59	NA	11.7
7	16 mg/100 μCi <sup>c</sup>	TRA	6	NC	240	0.18	2.41	6.92	100
		Emvododstat	3	79	240	0.14	1.58	2.46	35.6
		O-Desmethyl emvododstat	6	43	144	0.016	0.25	0.60	8.61
		M298	240	NC	240	0.002	NC	0.32	4.66
	M312	240	NC	240	0.001	NC	0.30	4.31	
		M443	144	NC	240	0.005	0.06	1.04	15.0
		M474	240	NC	240	0.004	0.02	0.51	7.41
		O-Desmethyl emvododstat glucuronide	6	58	240	0.025	0.33	0.81	11.7

AUC<sub>0-24</sub>, area under the plasma concentration-time curve from time zero to 24 hours postdose; AUC<sub>0-240</sub>, area under the plasma concentration-time curve from time zero to 240 hours postdose; NA, not applicable; NC, not calculable

oral dose) but was much higher, 6% of the dose by 240 hours postdose and up to 37% of the dose extrapolated to infinity, in human subjects (Table 4).

Since the metabolism of emvododstat in humans appears to be time dependent (Bender Ignacio et al., 2016), a study design with a 6-day once-daily 16 mg/0.3 μCi oral dosing followed by a 16 mg/100 μCi oral dose was adopted to evaluate mass balance and emvododstat metabolism near the steady state. Similar metabolite profiles were observed between Day 6 and Day 7 in all matrices following repeat once-daily oral dosing of 16 mg/0.3 μCi <sup>14</sup>C-emvododstat for 6 days or following a single oral 16 mg/100 μCi <sup>14</sup>C-emvododstat dose on Day 7. Following the last 16 mg/0.3 μCi <sup>14</sup>C-emvododstat oral dose on Day 6, emvododstat was the dominant component in plasma, accounting for 51.0% of TRA in the 0-24-hour plasma pool, whereas M443, O-desmethyl emvododstat glucuronide, and O-desmethyl emvododstat, accounting for 14.1%, 11.7%, and 9.6% of TRA, respectively, were the most abundant metabolites in 0-24-hour plasma after the last 16 mg/0.3 μCi dose on Day 6. Other metabolites were much less abundant, each accounting for less than 4% of the 0-24-hour plasma radioactivity (Table 2). Emvododstat was not detectable, whereas M474, accounting for 72.5% of TRA, was the dominant metabolite in 0-24-hour urine on Day 6. Emvododstat and O-desmethyl emvododstat were the most abundant components, accounting for 20.3% and 47.2% of TRA, respectively, in 0-24-hour feces on Day 6 (Table 3). Following a 16 mg/100 μCi <sup>14</sup>C-emvododstat oral dose on Day 7, unchanged emvododstat was the most abundant circulating entity, accounting for 35.6% of AUC of 0-240-hour plasma TRA; M443 and O-desmethyl emvododstat glucuronide were the most abundant metabolites, accounting for 15.0% and 11.7% of plasma TRA, respectively; and O-desmethyl emvododstat, M474, M298, and M312 were less abundant metabolites, accounting for 8.61%, 7.41%, 4.66%, and 4.31% of AUC from time zero to 240 hours postdose TRA, respectively (Table 2). In 0-240-hour urine, emvododstat was not detectable, and M474 was the most abundant metabolite, accounting for 4.06% of the dose (Table 3). In 0-240-hour feces, emvododstat accounted for 1.63% of the dose, and O-desmethyl emvododstat was the most abundant metabolite, accounting for 8.97% of the dose; the other metabolites M298, M443, M312, and M324 were less abundant, accounting for 1.15%, 1.09%, 0.76%, and 0.50% of the dose, respectively (Table 3).

TABLE 3 Distribution of emvododstat and its metabolites in pooled Day-6 0-24-hour urine and feces following repeat once-daily oral dosing of 16 mg/0.3 μCi or 11.1 kBq <sup>14</sup>C-emvododstat for 6 days and in pooled 0-240-hour urine and feces following a 16 mg/100 μCi or 3.7 MBq <sup>14</sup>C-emvododstat dose on Day 7 in healthy male human

	Day 6 (0–24 h) <sup>a</sup> Radioactivity %		Day 7 (0–240 h) <sup>b</sup>					
			Radioactivity %		Dose %			
Metabolite	Urine	Feces	Urine	Feces	Urine (6%)	Feces (19.9%)	Total (25.9%)	
Emvododstat	ND	20.3	ND	8.18	ND	1.63	1.63	
O-Desmethyl emvododstat	ND	47.2	ND	45.1	ND	8.97	8.97	
M298	2.5	4.2	5.19	5.79	0.31	1.15	1.46	
M312	ND	7.8	ND	3.82	ND	0.76	0.76	
M324	1.2	3.2	ND	2.51	ND	0.50	0.50	
M443	0.9	5.4	ND	5.50	ND	1.09	1.09	
M474	72.5	ND	67.7	Trace	4.06	Trace	4.06	
M482	ND	1.4	ND	ND	ND	ND	ND	
O-Desmethyl emvododstat glucuronide	ND	0.6	ND	ND	ND	ND	ND	

<sup>&</sup>lt;sup>a</sup>AUC<sub>0-24</sub> TRA for Day 6 and AUC<sub>0-240</sub> TRA for Day 7

<sup>\*</sup>Repeat once-daily oral dosing of 16 mg/0.3 μCi or 11.1 kBq <sup>14</sup>C-emvododstat for 6 days.

\*Single oral 16 mg/100 μCi or 3.7 MBq <sup>14</sup>C-emvododstat dose on Day 7, which was preceded by repeat once-daily oral dosing of 16 mg/0.3 μCi or 11.1 kBq <sup>14</sup>C-emvododstat for 6 days.

<sup>&</sup>lt;sup>a</sup>Repeat once-daily oral dosing of 16 mg/0.3 μCi or 11.1 kBq <sup>14</sup>C-emvododstat for 6 days.

<sup>&</sup>lt;sup>b</sup>Single oral 16 mg/100 μCi or 3.7 MBq <sup>14</sup>C-emvododstat dose on Day 7, which was preceded by a 6-day repeat once-daily oral dosing of 16 mg/0.3 μCi or 11.1 kBq <sup>14</sup>C-emvododstat.

TABLE 4 Percentage of the administered dose recovered following a 16 mg/100 μCi or 3.7 MBq oral dose of <sup>14</sup>C-emvododstat on Day 7 in healthy male human subjects

	Time	Mean ± S.I	Mean ± S.D. Percentage of Dose Recovered				
Dose	Interval (h)	Urine	Feces	Total			
16 mg/100 μCi	$0-240^a \ 0-\infty^b$	$6.0 \pm 2.1$ 37.3 ± 2.9°	19.9 ± 3.5 56.6 ± 15.7 <sup>d</sup>	$25.9 \pm 5.1$ $94.7 \pm 15.6^d$			

It should be noted that except for O-desmethyl emvododstat and its glucuronide, both peaking at 6 hours postdose, formation of all other metabolites was slow, with T<sub>max</sub> observed from 144 to 240 hours following a single oral 16 mg/100 µCi dose on Day 7 in human subjects (Table 2). Due to slow elimination of TRA as observed from 36 to 240 hours postdose, concentrations of these slowly forming metabolites were low and were therefore hard to accurately measure using the scintillation counting approach. For this end, it is advantageous that metabolites were enriched after a 6-day repeat daily microtracer radioactivity dosing and quantified using the most sensitive AMS detection technique in combination with the plasma AUC pooling strategy (Hop et al., 1998). For example, M443, M312, and M298 were not detectable or barely detectable by liquid scintillation counting within 24 hours after a single high-radioactivity dose on Day 7 but can be adequately detected by AMS in 0-24-hour plasma following repeat daily microtracer radioactivity doses for 6 days (Table 2). A followup high-radioactivity dose on Day 7 provided the desired mass balance data and, most importantly, the plasma metabolite kinetics, generating useful and complementary distribution results for the Day-6 plasma metabolite data.

As noted above, different radioactivity detection techniques were used to analyze samples following the Day-6 microtracer radioactivity dose and the Day-7 high-radioactivity dose: after the last microtracer radioactivity dosing on Day 6, one plasma AUC pool, one urine pool, and one feces pool from all subjects were profiled using AMS technology, whereas pooled plasma at individual timepoints and one pooled urine and one pooled feces from all subjects were analyzed using traditional scintillation counting techniques. Compared with the highradioactivity dose (100 µCi) on Day 7, the microtracer dose (0.3 µCi/day) is negligible, and the resulting radioactivity after repeated dosing is too low to be detected by less sensitive

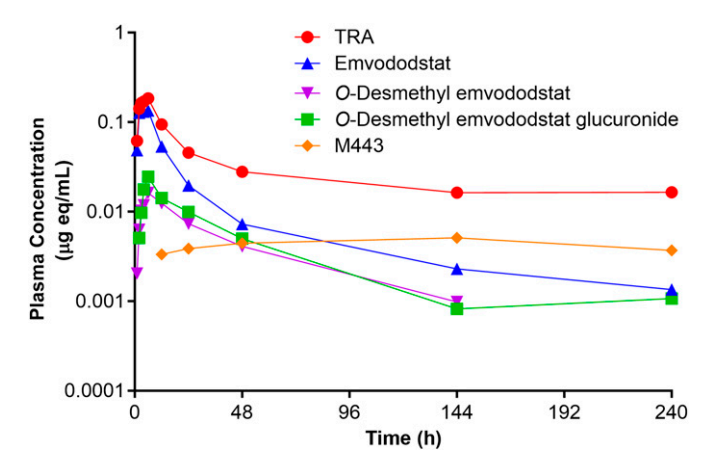


Fig. 4. Concentration-time curves of total radioactivity (TRA), emvododstat and its prominent metabolites in pooled plasma following a 16 mg/100  $\mu$ Ci or 3.7 MBq oral dose of emvododstat on Day 7 in male healthy subjects.

scintillation counting technique, and thus the Day-7 dose is considered a single dose that the plasma radioactivity was lower in Day-7 plasma than in Day-6 plasma (Fig. 2). Although the profiles are qualitatively similar to each other for each matrix obtained after the last microtracer radioactivity dose on Day 6 and after the high-radioactivity dose on Day 7, we believe the differences of relative abundance between the two profiles are largely due to repeat dosing versus single dosing, but other factors, such as analytical method used and sample pooling strategy (AUC pool versus individual timepoint plasma pool and 0-24-hour pool for Day-6 samples versus 0-240-hour pool for samples after Day-7 dose) cannot be excluded. A head-to-head comparison using AMS analysis on diluted Day-7 samples might provide additional information in this regard.

In other clinical studies that used similar daily oral doses, both emvododstat and O-desmethyl emvododstat reached steady state in approximately 2 weeks; therefore, steady state may not have been reached after six daily doses in the current study. Due to the limitation of tedious sample processing and long analysis time in the AMS analysis, similar to plasma sample analysis, urine and fecal samples were analyzed using different methods; therefore, the differences between Day-6 and Day-7 profiles may also be contributed to by analytical methods as well as by dosing frequency. Therefore, additional head-to-head sample analysis is needed to get a clear answer. Nevertheless, the current study design clearly shows the added value of repeated microtracer radioactivity dosing for drugs with slow metabolism and disposition, where steady state metabolite profiles might be different from single-dose metabolite profiles. The new FDA mass balance guidance suggests that one could employ a single radiolabeled dose of the investigational drug after reaching steady state with nonradiolabeled doses for such drugs. Because this approach only evaluates the clearance pathway of the radiolabeled drug, bioanalysis of the nonradiolabeled moieties at steady state should be conducted to help interpret the results (https://www.fda.gov/regulatoryinformation/search-fda-guidance-documents/clinical-pharmacologyconsiderations-human-radiolabeled-mass-balance-studies). However, bioanalytical methods may not be available for all moieties, especially if such studies are conducted at the early stage as the FDA advocated in that same draft guidance. On the other hand, quantification of nonradiolabeled moieties is not possible if the metabolites are not ambiguously identified or if the reference standards of the known metabolites are not available. In such situations, the repeated microtracer radioactivity dose study design may be a better choice to allow for full metabolite profiling at or near steady state if the drug or metabolite exhibits time-dependent pharmacokinetics, without the need for nonradiolabeled metabolite synthesis and bioanalytical method development. In our opinion, such design may be considered for other investigational drugs that show slow metabolism or for which metabolite formation is time dependent.

Theoretically, the amount of drug input equals the amount of drug excretion during the same dosing period at true steady state. If one is able to dose the subject close to the true steady state, and obtain all needed data (e.g., plasma PK based on individual timepoints and mass balance, etc.) after the last microtracer radioactivity dosing using more sensitive but costly AMS analysis, then the high-radioactivity dose may be optional, and the only advantage of such a dose is to obtain excretion kinetics if the elimination of radioactivity is slow like in our current study. Obviously, more research is needed to optimize such study designs and to maximize outcomes with a reasonable use of resources.

Following a single oral dose of <sup>14</sup>C-emvododstat in rats and dogs, emvododstat was the dominant radioactive component in rat plasma, whereas emvododstat and its two metabolites (O-desmethyl emvododstat and M312) were the major circulating components in dog plasma (Ma et al., 2022b). Although O-demethylation followed by glucuronidation

<sup>&</sup>lt;sup>b</sup>Extrapolated to infinity based on excretion rate constant

 $<sup>{}^{</sup>c}N = 4.$   ${}^{d}N = 3.$ 

are the common pathways in rats, dogs, and humans, the *N*-carbamoyl ester link was stable in rats but labile in dogs and humans: hydrolysis on the amide side led to the formation of M312 and subsequently M324, M298, and M474 in dogs and humans, whereas hydrolysis or transesterification on the ester side resulted in the formation of M443 in humans.

Liquid Chromatography/Mass Spectrometry (LC/MS) data indicate that M443 is a serine conjugate metabolite of emvododstat, possibly through the transesterification mechanism. Serine is a nonessential amino acid that is the precursor for cysteine, selenocysteine, tryptophan, glycine, and phospholipids and plays a role in the biosynthesis of purines and pyrimidines (Reitzer, 2009). Serine conjugates with xenobiotics (Steventon and Hutt, 2002; van Ravenzwaay et al., 2003; Aloysius et al., 2008) and endogenous serine conjugates with lipids such as *N*-arachidonoyl-serine (Milman et al., 2006) and *N*-stearoyl serine (Tan et al., 2010) have been reported in animal species, but the formation of serine conjugate metabolites of xenobiotics in humans seems to be rare. Nevertheless, additional research is needed to better understand the formation of M443 and the relevance of emvododstat metabolites to the efficacy and safety of emvododstat in humans.

In conclusion, since the metabolism and pharmacokinetics of emvododstat in humans is time dependent, the absorption, metabolism, and excretion of emvododstat were investigated by using a combination approach of microtracer radioactivity and high-radioactivity doses. The resolution of challenges due to slow metabolism and elimination of a lipophilic compound highlighted in this study was achieved by repeat daily microtracer radioactivity oral dosing followed by high-radioactivity oral dosing at therapeutically relevant doses. Such a design may provide an alternative approach to better understanding AME properties of investigational drugs that show slow metabolism or for which metabolite formation is time dependent.

#### **Data Availability**

The authors declare that all the data supporting the findings of this study are contained within the paper.

#### **Authorship Contributions**

Participated in research design: Ma, Laskin, Roffel, Vaes, O'Keefe, Golden, Kong.

Conducted experiments: Ma, Kong. Performed data analysis: Ma, Kong.

Wrote or contributed to the writing of the manuscript: Ma, Laskin, Roffel, Vaes, Tang, Kolnaar, Golden, Kong.

#### References

Aloysius HA, Elipe MVS, Arison BH, Faidley TD, Michael BF, Blizzard TA, Thompson DR, Shoop WL, and Tschirret-Guth RA (2008) Comparative disposition and metabolism of paraherquamide in sheep, gerbils, and dogs. *Drug Metab Dispos* 36:1659–1669.

Bender Ignacio RA, Lee JY, Rudek MA, Dittmer DP, Ambinder RF, and Krown SE; AIDS Malignancy Consortium (AMC)-059 Study Team (2016) Brief Report: A Phase 1b/Pharmacokinetic Trial of PTC299, a Novel PostTranscriptional VEGF Inhibitor, for AIDS-Related Kaposi's Sarcoma: AIDS Malignancy Consortium Trial 059. J Acquir Immune Defic Syndr 72:52-57.

Branstrom A, Cao L, Furia B, Trotta C, Santaguida M, Graci JD, Colacino JM, Ray B, Li W, Sheedy J, et al. (2022) Emvododstat, a potent dihydroorotate dehydrogenase inhibitor, is effective in preclinical models of acute myeloid leukemia. Front Oncol 12:832816.

Cao L, Weetall M, Bombard J, Qi H, Arasu T, Lennox W, Hedrick J, Sheedy J, Risher N, Brooks PC, et al. (2016) Discovery of novel small molecule inhibitors of VEGF expression in tumor cells using a cell-based high throughput screening platform. PLoS One 11:e0168366.

Cao L, Weetall M, Trotta C, Cintron K, Ma J, Kim MJ, Furia B, Romfo C, Graci JD, Li W, et al. (2019) Targeting of hematologic malignancies with PTC299, a novel potent inhibitor of dihydroorotate dehydrogenase with favorable pharmaceutical properties. *Mol Cancer Ther* 18:3–16.

Hop CECA, Wang Z, Chen Q, and Kwei G (1998) Plasma-pooling methods to increase throughput for in vivo pharmacokinetic screening. J Pharm Sci 87:901–903.

Luban J, Sattler RA, Mühlberger E, Graci JD, Cao L, Weetall M, Trotta C, Colacino JM, Bavari S, Strambio-De-Castillia C, et al. (2021) The DHODH inhibitor PTC299 arrests SARS-CoV-2 replication and suppresses induction of inflammatory cytokines. Virus Res 292:198246.

Ma J, Kaushik D, Yeh S, Northcutt V, Babiak J, Risher N, Weetall M, Moon YC, Welch EM, Molony L, et al. (2022a) In vitro metabolism, pharmacokinetics and drug interaction potentials of emvododstat, a DHODH inhibitor. Xenobiotica 52:152–164.

Ma J, Ye Q, Northeutt V, Babiak J, and Kong R (2022b) Absorption, distribution, metabolism and excretion of <sup>14</sup>C-Emvododstat following a single oral dose in rats and dogs. *Xenobiotica* 52:1031–1040.

Milman G, Maor Y, Abu-Lafi S, Horowitz M, Gallily R, Batkai S, Mo FM, Offertaler L, Pacher P, Kunos G, et al. (2006) *N*-arachidonoyl L-serine, an endocannabinoid-like brain constituent with vasodilatory properties. *Proc Natl Acad Sci USA* 103:2428–2433.

Packer RJ, Rood BR, Turner DC, Stewart CF, Fisher M, Smith C, Young-Pouissant T, Goldman S, Lulla R, Banerjee A, et al. (2015) Phase I and pharmacokinetic trial of PTC299 in pediatric patients with refractory or recurrent central nervous system tumors: a PBTC study. J Neurooncol 121:217–224.

van Ravenzwaay B, Hardwick TD, Needham D, Pethen S, and Lappin GJ (2003) Comparative metabolism of 2,4-dichlorophenoxyacetic acid (2,4-D) in rat and dog. Xenobiotica 33:805–821.

Reitzer L (2009) Amino acid synthesis in, Encyclopedia of Microbiology (Schaechter M ed), 3rd ed, pp 1–17, Academic Press, Oxford, UK.

Steventon GB and Hutt AJ (2002) The amino acid conjugations, in *Enzyme Systems that Metabolise Drugs and Other Xenobiotics* (Ioannides C ed) pp 504–506, John Wiley & Sons Ltd, West Sussex, UK.

Tan B, O'Dell DK, Yu YW, Monn MF, Hughes HV, Burstein S, and Walker JM (2010) Identification of endogenous acyl amino acids based on a targeted lipidomics approach. J Lipid Res 51:112–119.

van Duijn E, Sandman H, Grossouw D, Mocking JA, Coulier L, and Vaes WH (2014) Automated combustion accelerator mass spectrometry for the analysis of biomedical samples in the low attomole range. Anal Chem 86:7635–7641.

Weetall M, Davis T, Elfring G, Northcutt V, Cao L, Moon YC, Riebling P, Dali M, Hirawat S, Babiak J, et al. (2016) Phase 1 study of safety, tolerability, and pharmacokinetics of PTC299, an inhibitor of stress-regulated protein translation. Clin Pharmacol Drug Dev 5:296–305.

Address correspondence to: Dr. Ronald Kong, PTC Therapeutics Inc. 100 Corporate Court, South Plainfield, New Jersey 07080. E-mail: rkong@ptcbio.com